JOURNAL OF CATALYSIS 78, 51–76 (1982)

Catalytic Activity of Mixed Copper Chlorides ($CuCl_x$, $1 \leq x \leq 2$)

2. ESR, IR, and Mechanistic Studies of Dehydrochlorination of *tert*-Butyl Chloride

C. F. NG,[1] K. S. LEUNG, AND C. K. CHAN

Department of Chemistry, University of Hong Kong, Hong Kong

Received January 13, 1982; revised June 1, 1982

A study of the surface species present in the *tert*-butyl chloride/$CuCl_x$ system using ESR and ir techniques was attempted. ESR data revealed that treatments of CuCl by *tert*-butyl chloride led to the generation of three paramagnetic species with g values 2.004 (b), 2.003 (c), and 2.092 (a′), respectively, in addition to the one inherent in the "virgin" sample, viz. signal (a): $g_\perp = 2.251$, $g_\parallel = 2.056$. These species were found to undergo change at various conditions. It was also shown that species (a′) and (b) clearly participated in dehydrochlorination. The nature of these species is suggested to be (a) Cu_s^{2+} under the influence of O^{2-} and Cl^- ions, (b) $Cl_{in(s)}^{\cdot}$, (c) $\square_{Cu}+$, and (a′) Cu^{2+} ions distributed rather closely in certain parts of the CuCl lattice. Present ir studies appear to establish the existence of a *tert*-butyl group bonded to a surface copper ion on both CuCl and $CuCl_2$ surfaces during dehydrochlorination of *tert*-butyl chloride. The effects of the surfaces on absorption frequencies of this group are discussed. Infrared data also suggest the presence of a surface hydrogen bonded to a chloride ion and to a copper ion on CuCl and $CuCl_2$ surfaces, respectively, during dehydrochlorination. On the basis of ESR and ir findings, kinetic analysis, and other types of information hitherto available, two different mechanisms operating in various ranges of composition were proposed, one associated with a triangular active center involving $Cu_{F(s)}^{+}$ in the $CuCl_2$ phase, and the other associated with a triangular active center involving $Cl_{in(s)}^{\cdot}$ in the CuCl phase. These defect mechanisms are quite different from that exhibited by ordinary polar catalysts.

INTRODUCTION

In Part I of this work (*1*), it was established that the catalytic activity of $CuCl_x$ toward dehydrochlorination of *tert*-butyl chloride (tbc) could be correlated with the amount of Cu_F^+ ions migrated from the CuCl to the $CuCl_2$ phase. Moreover, on the basis of values of apparent order and apparent activation energy it was concluded that at least two mechanisms are operating at different composition ranges of $CuCl_x$. It appeared therefore that a study of the surface species occurring in the tbc/CuCl and tbc/$CuCl_2$ systems by ESR and ir techniques may be useful in the further elucidation of the dehydrochlorination mechanisms which obviously involve defects, in contrast to those normally described for elimination reactions on polar catalysts (see, e.g., Ref. (*2*)).

[1] To whom correspondence should be addressed.

The ESR study was limited to the CuCl sample only because $CuCl_2$ was shown (*3*) to give a very broad and featureless ESR signal which would therefore mask smaller signals, if any, present in the system. Since the Cu^{1+} ion does not exhibit an ESR spectrum, the ESR spectra observed in this work for a CuCl sample under various conditions would necessarily owe their origins to impurities, or point defects, or surface species arising from gas adsorption. As for ir study, both CuCl and $CuCl_2$ systems were investigated. Moreover, to help ascertain the possible intermediates in the dehydrochlorination of tbc on $CuCl_x$, the ir spectra of adsorbed isobutene, H_2O, and D_2O on the two solids were also studied in addition to those of adsorbed tbc. Both solids had low transmission in the infrared, so spectra accumulations were necessitated.

We shall first attempt to establish the surface species present in the tbc/CuCl and

0021-9517/82/110051-26$02.00/0
Copyright © 1982 by Academic Press, Inc.
All rights of reproduction in any form reserved.

tbc/$CuCl_2$ systems and then to deduce the mechanisms of tbc dehydrochlorination on $CuCl_x$ on the basis of information hitherto available.

EXPERIMENTAL

Kinetic Method

The experimental equipment and techniques for sample preparation and purification, and kinetic measurements have been reported in Part I (*1*). To establish rate equations, some of the runs were carried out for a long period and some were even allowed to reach equilibrium.

ESR Method

The spectrometer used is JEOL No. JES-FE3X X-band ESR spectrometer equipped with a variable temperature unit, made available to us by Chinese University of Hong Kong. The ESR tube containing the catalyst was evacuated and baked at ~393 K in 10^{-5}–10^{-6} τ for 3 hr prior to admission of tbc. Measurements were taken immediately and at frequent intervals for a certain period. However, no simultaneous *in situ* pressure change measurements were attempted. The details of the apparatus are described elsewhere (*4*). Most of the measurements were made at 383 K, the reaction temperature. Spin density was estimated using a known amount of 10 mol% $MnSO_4$ in $MgSO_4$ crystals.

IR Method

Apparatus. The infrared spectrophotometer used is a Perkin-Elmer Model 577 with grating optics. It is coupled to a home-built accumulation system with an interface unit. The accumulation system consists of an accumulator and a wavenumber selection unit. The former is a Northern Scientific NS-560 signal average computer (a multichannel analyzer of capacity 2K). The latter makes use of an optical cell and a decoder. For this purpose, the rotating drum for wavenumber change is covered by a reflecting white disc graded with black lines. Thus when the drum (disc) rotates, the optical cell will generate a sequence of pulse signals the number of which can be counted by a decoder. The degree of rotation of the drum and hence the wavenumber range can then be controlled.

A T-shaped sample cell was used. It is 10 cm in length with NaCl windows sealed to a flanged pyrex cell body by high vacuum silicon grease and Araldite. The cell was so built as to allow for a home-made ceramic sample holder to move freely in its vertical section (~17 cm in height). Such movement enables the sample to be heated at the far end of the vertical section whereas its ir spectra to be measured in the center of the cell, i.e., the other extremity of the vertical section. The cell with solid samples could be evacuated through a sidearm and joint by a vacuum system to a dynamic vacuum of $\sim 4 \times 10^{-6}$ Torr at room temperature. The reference cell used is similar to the sample cell except that it does not cater to sample heating. The two could be connected through joints so that gas pressure in both cells could be equalized.

Procedures. Preparation of sample pellets: A powder sample (0.2–0.3 g) was grounded and transferred to a 2-cm die assembly in a dry box. The assembly was subsequently removed and placed in a hydraulic press. A pressure of 14 tons was applied for 5 min. The pellet so obtained was about 0.5–1 mm thick, fairly light colored for CuCl, and brownish for $CuCl_2$.

Measurements of ir spectra: The pellet sample after being charged into the sample cell was first evacuated and generally baked at 403 K (for water adsorption study, a higher temperature was used) in the vertical section for 5 hr to $\sim 1 \times 10^{-5}$ Torr. Afterward, the vertical section was adjusted to the required adsorption temperature. Gas was then admitted into the cell to a required pressure. After about 30 to 60 min of contact with gas, the sample was quenched to room temperature. The sample holder was then inverted to the center of the cell. The

pressure of the sample cell was reduced gradually to ~0.5 Torr and then connected to the reference cell for equalization of pressure. The room temperature ir spectra of the sample were then measured with a suitable choice of wavenumber range and number of accumulation times.

Materials. Apart from copper chloride samples the tbc which have been described in Part I (*1*), isobutene and D_2O were also involved in the ir work. The former was Matheson Gas products, R.P. grade, dried by phosphorous pentoxide before use. The latter was from Merck with minimum isotopic purity 99.7 atm% D, used without further purification.

RESULTS

Before the results are presented, the conditions of the samples should first be made clear.

From earlier kinetic data, it was found that the reaction rate of a given $CuCl_x$ sample was generally higher in the first run and reached a constant level after one to three runs. The rate data reported were indeed those runs after a constant rate was attained. In view of this, it was deemed necessary to define the conditions of the samples in ESR and ir studies so that results could be properly compared.

A "virgin" sample therefore refers to one which has undergone all necessary chemical treatments, followed by baking at elevated temperature (383–403 K) and evacuating to $\sim 1 \times 10^{-5}$ Torr for several hours. Such a sample should be the one on which the initial kinetic run is to be taken. An "equilibrated" sample, on the other hand, refers to the one for which the sample has been subjected to several tbc treatments until spurious ir peaks or ESR signals as described later disappeared. Such a sample should then correspond to that for which the rate of reaction has reached a constant level.

While the kinetic data for a nonequilibrated sample were not considered because of their lack of immediate interest and complexities, the ESR and ir data could be analyzed and provide certain relevant information as will be seen later.

I. ESR Study of the tbc/CuCl System

The ESR spectrum of CuCl after baking in high vacuum ("virgin" sample) showed a broad asymmetric signal (a) with $g_\perp = 2.251$, $g_\parallel = 2.056$, and peak to peak width 278 G and a very sharp signal (c) with $g = 2.003$, and width 1.8 G as shown in Fig. 1a. On treatment with tbc and subsequent evacuation and baking, signal (a) diminished in size while signal (c) remained almost constant. However, a new very slightly asymmetric signal (b) with $g_{av} = 2.004$ and width 5.8 G emerged and grew in magnitude after cycles of treatment with tbc, evacuation, and baking (Fig. 1b). After treatments of four to five times, the magnitude of signal (b) reached a maximum value, and at the same time signal (a) diminished to a very weak, broad, and slightly asymmetric signal (a′) as shown in Fig. 1c with $g = 2.092$ and width 444 G, resembling the $CuCl_2$ signal, whereas signal (c) became a small hump superimposing on signal (b). Actually, signal (a′) was already in the making immediately after treatment with tbc as can be seen from the shape of a signal (a) in Fig. 1b. At this stage, species (b) could be estimated to be $\sim 8 \times 10^{14}$ spins in the sample, approximately 10^{-4} mol%.

The characteristics of the various species are summarized in Table 1 whereas rough data for the effect of cyclic treatments with

TABLE 1

ESR Species in the *tert*-Butyl Chloride/CuCl System

Species	g values	Peak-to-peak width (Gauss)	Tentative assignment
(a)	$g_\perp = 2.251$ $g_\parallel = 2.056$	278	Cu_x^{2+} under influence of O^{2-} and Cl^- ions
(b)	2.004	5.8	$Cl_{int(s)}$
(c)	2.003	1.8	$\square_{Cu^+}$
(a′)	2.092	444	Cu^{2+} ions distributed rather closely in certain parts of CuCl lattice

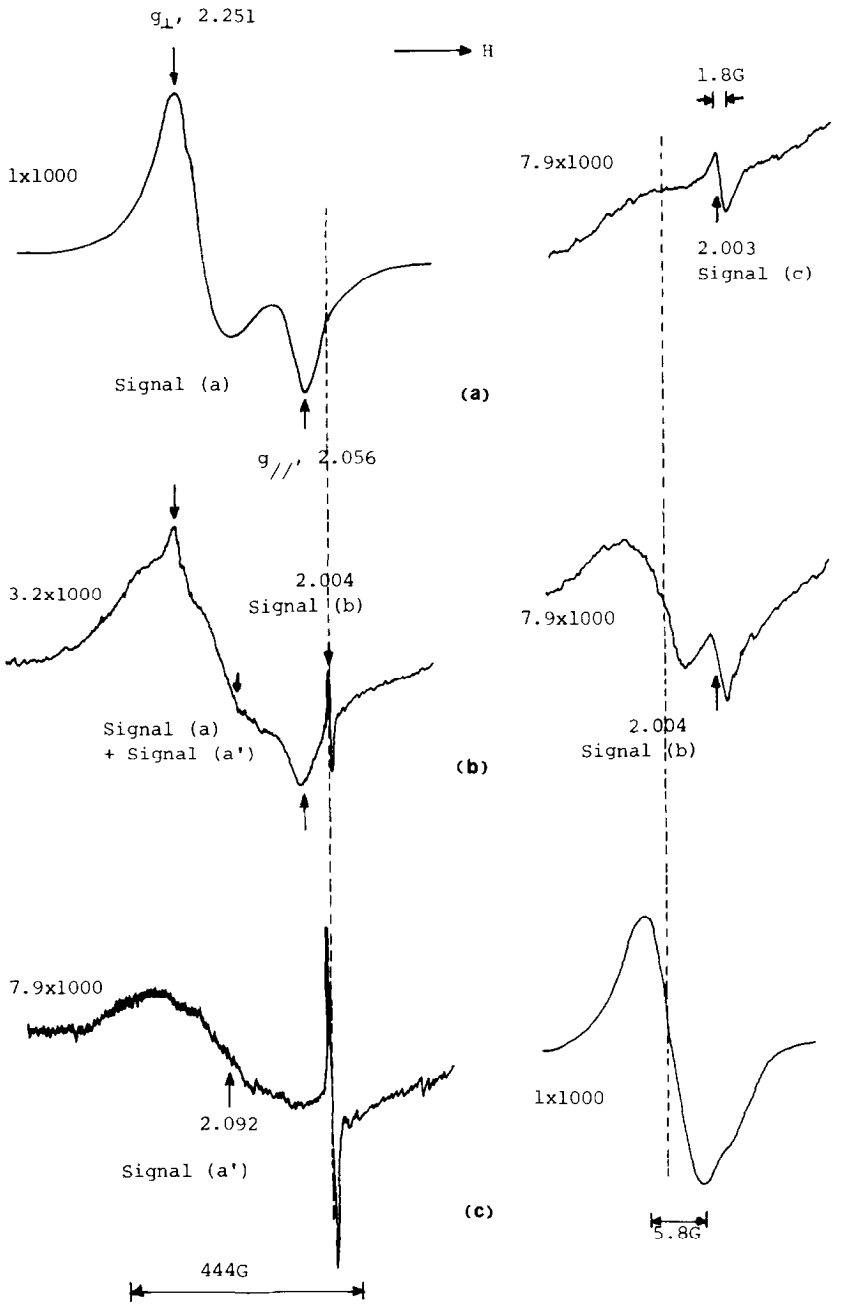

FIG. 1. ESR signals of fresh and tbc-treated CuCl. (a) Fresh, evacuated; (b) after tbc treatment once; (c) after tbc treatments four times.

tbc on the various species are shown in Table 2, where the value of a signal intensity is in terms of peak to peak height for a particular attenuation of the spectrometer. Attempts were also made to look for hyperfine structures at low temperature. However, no hyperfine structure was observed for all signals at temperature as low as 163 K.

After four to five tbc treatments, usually no more significant change was found in the overall spectrum and the surface in such a state could be regarded to be "equili-

TABLE 2

Variations of Signals on Treating Fresh CuCl with *tert*-Butyl Chloride

No. of treatments	Relative magnitude of signals		
	a	b	c
(1) Evacuated background	276.0	—	5.01
tbc in	231.0	1.02	5.10
After 60 min	243.0	2.30	5.00
(2) Evacuated background	248.0	5.19	5.03
tbc in	220.0	6.96	5.00
After 60 min	228.0	8.86	4.98
(3) Evacuated background	232.0	26.40	3.26
tbc in	186.0	30.50	3.54
After 60 min	192.0	35.50	3.44
(4) Evacuated background	116.0	60.70	2.40
tbc in	100.0	60.8	2.20
After 60 min	115.0	62.5	2.00
(5) Evacuated background	8.25	85.0	—
tbc in	8.10	65.0	—
After 60 min	4.13	60.3	—
	changed to a'		
(6) Evacuated background	2.00	83.5	—
tbc in	2.35	68.5	—
After 60 min	2.50	59.6	—

brated." Thus, *in situ* kinetic measurements were made at this stage. Figures 2 and 3 show the change of signal (a') and (b) for one of these runs. The broad signal (a') showed a definite though slight increase in magnitude, in spite of a relatively large experimental error involved as shown.

Rough vacuum had no pronounced effect on signal (b). However, baking at high vacuum restored the magnitude of (b) to a value more or less the same as the maximum value mentioned above. Thus this indicates that the species of signal (b) took part in the catalytic dehydrochlorination of *tert*-butyl chloride on CuCl at 383 K.

It may be appreciated that the foregoing data are not quantitative. The gaseous reactants and products were just in contact with the catalyst inside the narrow ESR tube and no circulation was applied for well mixing. Thus the kinetics would presumably suffer from the diffusion limitation of the gases and the rate of change of signals would not necessarily be the same as that expected during reactions studied in a static reactor.

II. IR Studies

A. Adsorption of tbc and Isobutene on CuCl

A CuCl sample showed characteristic peaks in the 750–950 cm^{-1} region. Figure 4 illustrates the change of the spectrum of a CuCl sample under various conditions in this region. Figure 4a is the spectrum of a CuCl sample which after baking at 383 K and evacuation to $\sim 10^{-5}$ Torr yielded Fig. 4b. Thus Fig. 4b corresponds to a CuCl sample in a "virgin" state. The three bands exhibited by the initial sample were retained though slightly diminishing in intensity in the "virgin" state. However, a comparison among Figs. 4a, b, c, d, and e suggests that the three bands could be effectively eliminated by treating with either tbc (Figs. 4c and d) or HCl (Fig. 4e). On the other hand, Figs. 4a, b, and f suggest that simply evacuating and heating at reaction temperatures only slightly reduced, but heating at 823 K could effectively eliminate the three bands in question. For subsequent ir adsorption work, samples with surface condition of Fig. 4d or f were used because they could be regarded as "equilibrated".

In comparison with the family of three bands above, Fig. 5 shows the spectra of products (liquids) trapped after tbc treatments. It can be seen that tbc treatments led to a parallel increase in absorption around 3560 and 1620 cm^{-1}.

Figure 6 shows the ir spectra of CuCl in the presence of tbc or isobutene over various spectral ranges. In case of tbc, the absorption bands observed in region (A), presumably arising from various C–H stretch modes, are most intense with the exception of a weak band at 2804 cm^{-1} that was observable only after adsorption at elevated temperature (Fig. 6b). The bands in regions (C) and (D) are also moderately intense. In region (B) and frequency range below region (D), no bands were detectable; this can

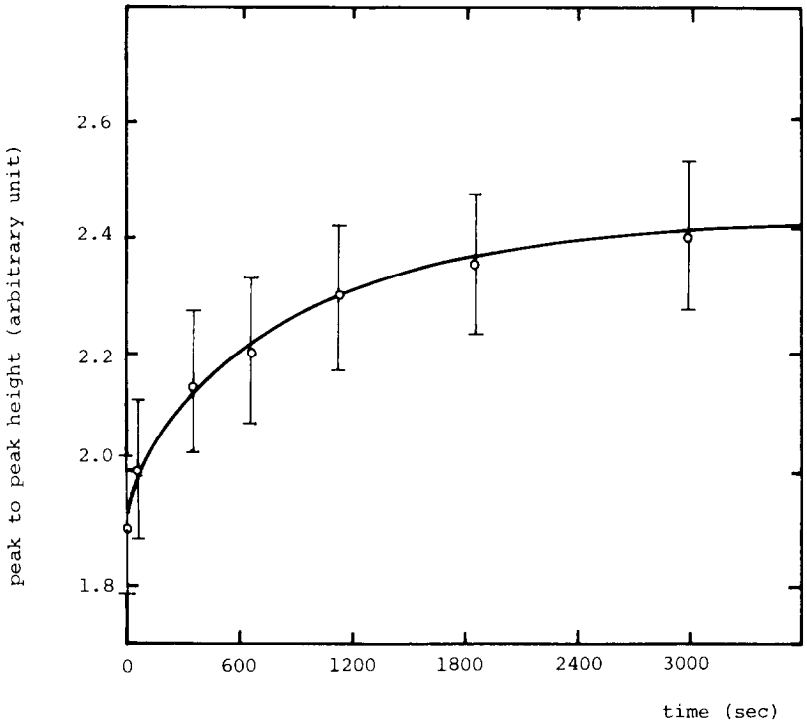

FIG. 2. Change of ESR signal (a') of CuCl in contact with tbc at 383 K.

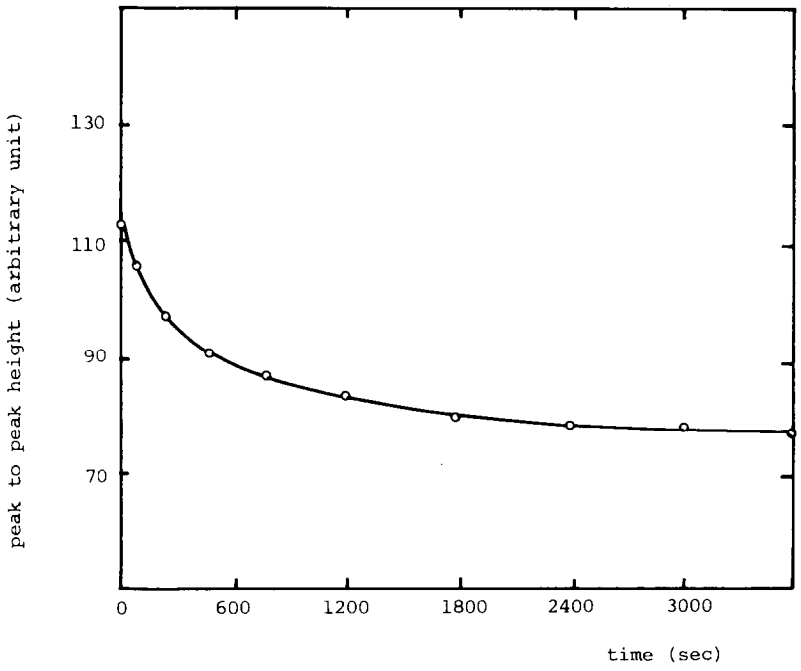

FIG. 3. Change of ESR signal (b) of CuCl in contact with tbc at 383 K.

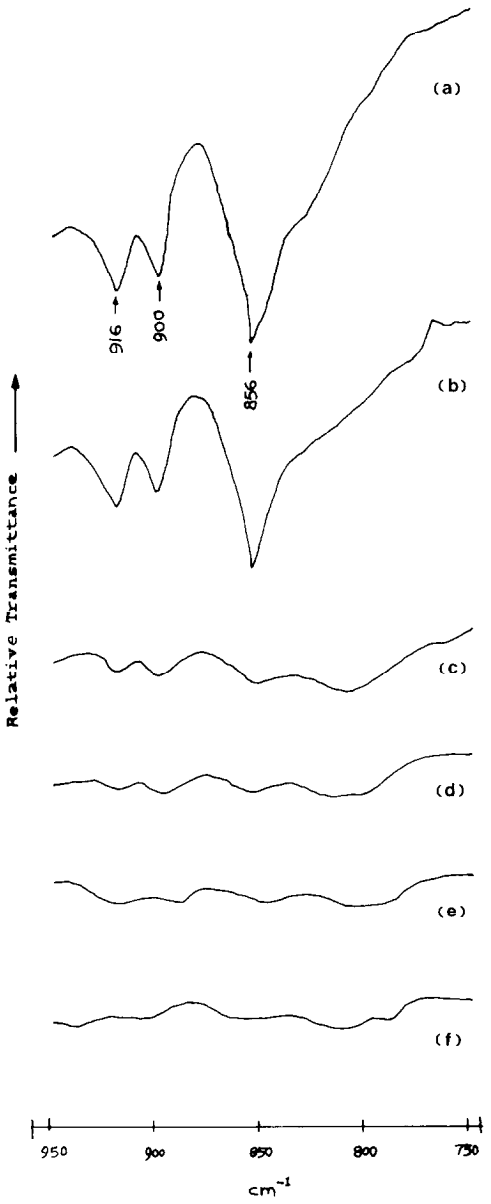

FIG. 4. Infrared spectra of CuCl under various conditions. (a) CuCl sample (×5). (b) Sample (a) after being pumped by diffusion pump for 2 hr at 393 K (×5) ("virgin"). (c) Sample pellet obtained from powder in stage (b) after treatment with 95 Torr tbc at 383 K for about 13 hr followed by rough pumping (×5). (d) Sample pellet obtained from powder in stage (c) after further treatment with 128 Torr tbc at 383 K for 8 hr followed by rough pumping (×5). (e) Sample pellet obtained from powder in stage (b) after treatment with 50 Torr HCl for about 5 hr followed by rough pumping (×5). (f) Sample pellet obtained from powder (a) after heating under dry nitrogen of 0.5 atmospheric pressure at 723 K in a sealed tube for a day (×5).

be compared with the spectrum in Fig. 6e which shows only one rather weak band around 886 cm^{-1}.

The positions and intensity of various peaks are summarized in Table 3 in which data of gaseous tbc and isobutene are also included for comparison.

B. Adsorption of tbc and Isobutene on $CuCl_2$

The background absorption and scattering of the brown $CuCl_2$ samples were generally much more severe than that of CuCl. Toward the low-frequency range, the background was particularly steep. Moreover, it was found that the magnitude of absorption bands in general is weaker than those in the CuCl case. Consequently, spectra were accumulated over narrower spectral ranges and a greater number of times.

Figure 7 shows ir spectra of $CuCl_2$ samples adsorbed with tbc or isobutene under various conditions. The absorption bands in

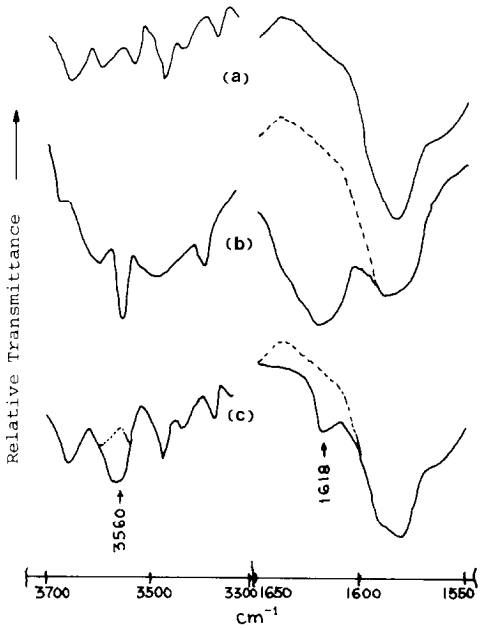

FIG. 5. Infrared spectra of trapped products after tbc treatments. (a) Background of the cell used for trapping products (×5). (b) Trapped products after one tbc treatment on CuCl (freshly washed) at 393K (×5). (c) Trapped products after a further tbc treatment on the same CuCl sample (×5).

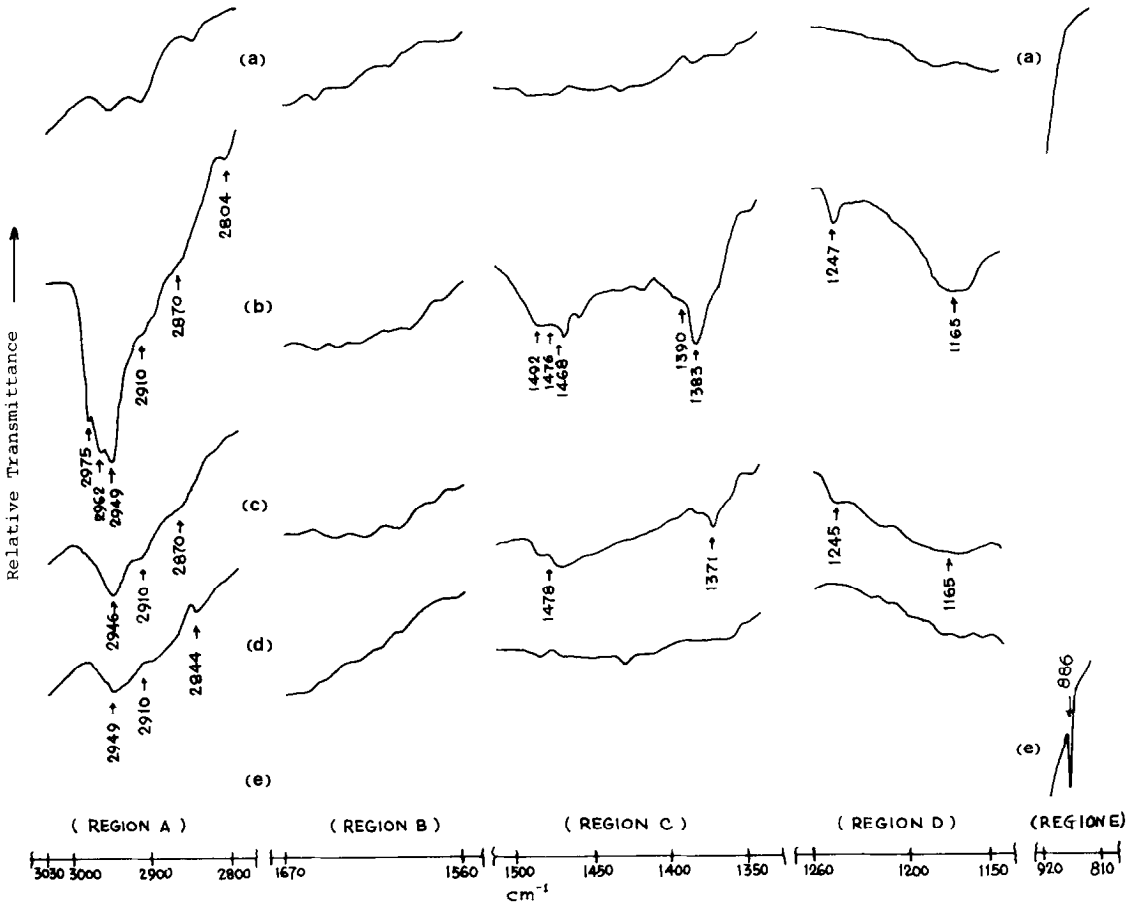

FIG. 6. Infrared spectra of CuCl with tbc and isobutene adsorptions (20 times spectra accumulation, each ×5). (a) "Virgin" CuCl ("background"). (b) "Virgin" CuCl after treatment with 120 Torr tbc at 393 K for 1 hr followed by quenching to RT and gradual pressure reduction in the cells to ~0.5 Torr. (c) CuCl in stage (b) evacuated by rotary pump to 10^{-4} Torr for 2 min. (d) "Virgin" CuCl after treatment with 120 Torr tbc at RT for 1 hr and gradual pressure reduction in the cells to ~0.5 Torr. (e) "Virgin" CuCl after treatment with 30 Torr isobutene at 393 K for 30 min followed by quenching to RT and gradual pressure reduction in the cells to ~0.5 Torr.

the C–H stretch region are again fairly intense but apparently rather complicated. In region (B), the background happened to have absorption bands presumably due to some trace of strongly retained water (either surface or lattice). Nevertheless, a close examination could reveal that absorption occurred at ~1626 and ~1585 cm^{-1}, respectively. To check where bands of adsorbed isobutene would lie, spectrum Fig. 7e was obtained. In region (A), four bands were observed. From the shape and position of the adsorbed tbc and adsorbed isobutene bands in region (B), one might see that the 1585 cm^{-1} band could well be due to adsorbed isobutene which was released as a product of elimination of tbc on $CuCl_2$ surface (recalling spectrum 7b was obtained by tbc adsorption at 393 K). In region (C), two bands were observed for adsorbed tbc and adsorbed isobutene. The former pair is slightly higher in frequency. In region (D),

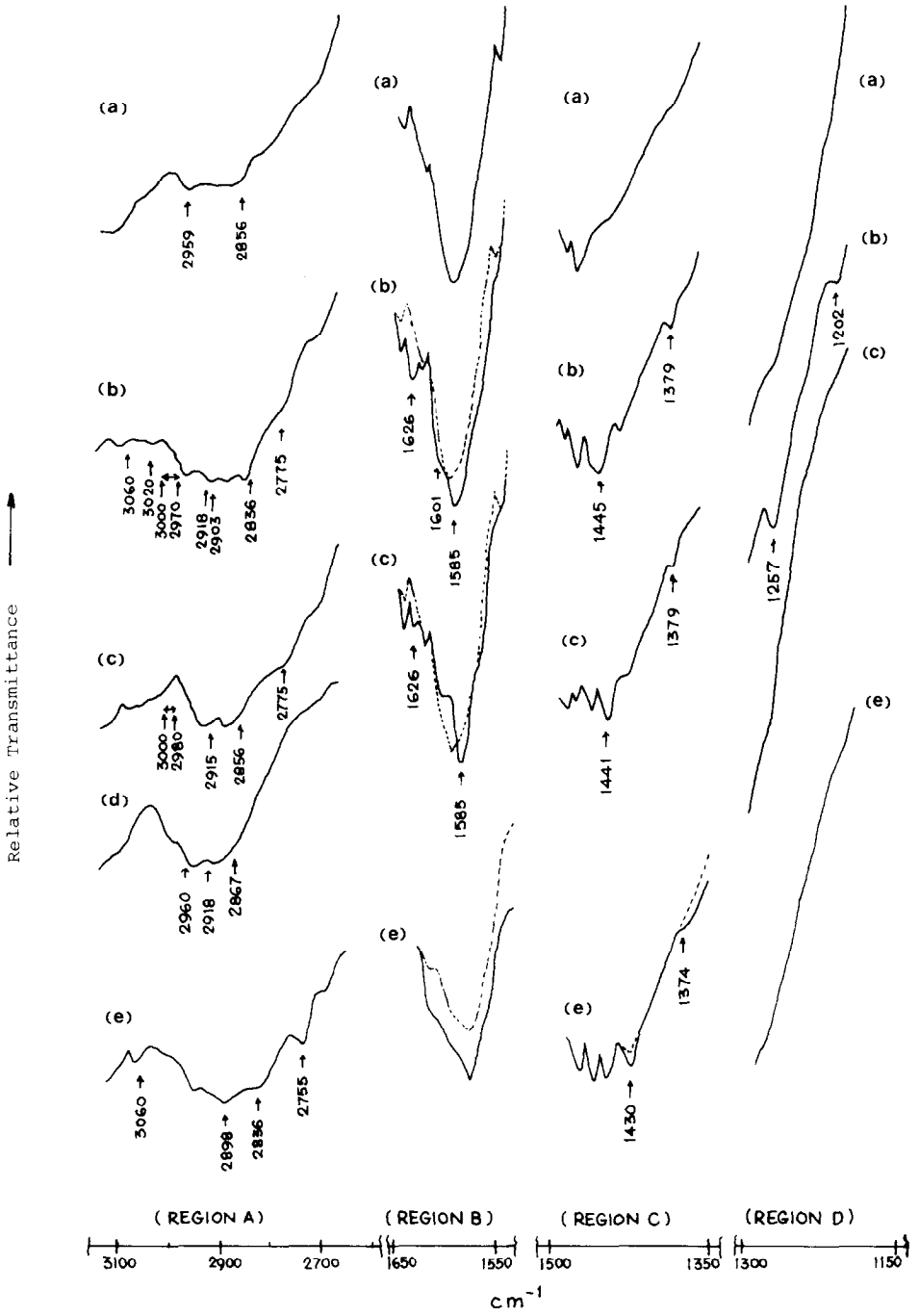

FIG. 7. Infrared spectra of $CuCl_2$ with tbc and isobutene adsorptions (10 times spectra accumulation in region A and 40 times in other regions, each ×5). (a) $CuCl_2$ baked at 393 K and pumped to 8×10^{-6} Torr ("virgin" sample, "background"). (b) $CuCl_2$ in stage (a) after treatment with 100 Torr tbc at 393 K for 45 min, followed by quenching to RT and gradual pressure reduction in the cells to ~0.5 Torr. (c) $CuCl_2$ in stage (b) evacuated by rotary pump to 10^{-4} Torr for 2 min. (d) "Virgin" $CuCl_2$ after treatment with 100 Torr tbc at RT for 45 min and gradual pressure reduction in the cells to ~0.5 Torr. (e) "Virgin" $CuCl_2$ after treatment with 20–30 Torr isobutene at 393 K for 45 min, followed by quenching to RT and gradual pressure reduction in the cells to ~0.5 Torr.

TABLE 3

Infrared Results of CuCl

Spectra	Region A (3080–2800 cm^{-1})	Region B (1820–1560 cm^{-1})	Region C (1500–1350 cm^{-1})	Region D (1300–1180 cm^{-1})	Region E (920–800 cm^{-1})
tbc (b − a)[a]	2975, (0.168)[b] 2962 (0.215) 2949, (0.233) 2910 (0.114) 2870, (0.100) 2804 (0.074)	—	1492, (0.021) 1468 (0.021) 1390, (0.025) 1383 (0.048)	1247, (0.015) 1165 (0.034)	—
tbc (c − a)[a]	2946, 2910	—	1478, 1371	1245, 1165	—
Isobutene	—	—	—	—	886
Gaseous tbc	2990, (vs sh) 2979 (vs sh) 2960, (ms) 2922 (ms) 2870 (m)		1479, (m) 1460 (m) 1385 (s)	1242, (m) 1161 (s)	812 (m)
Gaseous isobutene	3080, (s) 2960 (vs) 2940, (vs) 2890 (sh) 2740 (w)	1770, (m) 1660 (s)	1470, (s) 1460 (s) 1450, (vs) 1395 (s) 1385, (s) 1375 (sh)	1292, 1281, 1270 (m)	910, (s) 890, (vs) 872 (s)

[a] c–a, b–a, subtraction of a (background) from b and c, respectively.
[b] Figures in parentheses where given are relative absorbance.

two shoulders were observed for adsorbed tbc at ~1257 and ~1202 cm^{-1}, whereas no absorption band was detectable for adsorbed isobutene. The results are summarized in Table 4.

C. *Adsorption of H_2O and D_2O on CuCl and $CuCl_2$*

Since it was suspected that H_2O might be present on the surface of $CuCl_x$ for one reason or another, it therefore appeared desirable to ascertain the positions of absorption bands of adsorbed water, if any, especially in the angle bending region. To this end, adsorption of H_2O and D_2O was performed on CuCl as well as $CuCl_2$ samples. Figures 8 and 9 show the ir spectra of adsorbed H_2O and D_2O on CuCl and $CuCl_2$, respectively. While the D_2O bands could be unambiguously assigned in both cases, being 1196 and 1187 cm^{-1}, respectively, for CuCl and $CuCl_2$, the H_2O band could only be clearly recognized in the case of CuCl (~1638 cm^{-1}). For $CuCl_2$ the adsorbed H_2O band apparently overlaps with the background water band. The shape of the spectrum of the adsorbed H_2O vaguely indicates that the angle bending frequency of the adsorbed species would be around 1580–1600 cm^{-1}.

III. Kinetic Results

Dehydrochlorination of tbc is a reversible reaction. Catalytic activity expressed in terms of initial rate was already reported in Part I (*1*). One typical pressure time curve is shown in Fig. 10. The order of reaction was established by the initial rate method as illustrated in Fig. 11. The complete rate equation will be established from data of long period runs as described later.

TABLE 4

Infrared Results of $CuCl_2$

Spectra	Region A (3100–2600 cm^{-1})	Region B (1800–1550 cm^{-1})	Region C (1500–1350 cm^{-1})	Region D (1300–1150 cm^{-1})	Region E (1160–800 cm^{-1})
tbc (b − a)[a]	3060(sh),[b] 3000–2970(br s) 2918(s), 2836(s) 2775(*br sh*)	1626, 1601(vw sh) 1585	1445(br) 1379	1257, 1202(sh)	Not studied
tbc (c − a)[a]	3000–2980(br) 2915(w), 2856(w) 2775(v w)	1626 1580	1440(br) 1379(sh)	1257(sh), 1202(sh)	Not studied
tbc (*d* − a)[a]	2960(br sh), 2918(s) 2867(sh ?)	Not studied	Not studied	Not studied	Not studied
isobutene (e − a)[a]	3060(w), 2898(s) 2836(s), 2755(ms)	1580	1430 1374(br sh)	—	Not studied

[a] Subtracted from background spectrum a.

[b] In parentheses, description of bands where given is intended to give a very rough indication of intensity, applicable within the same group of bands *only*.

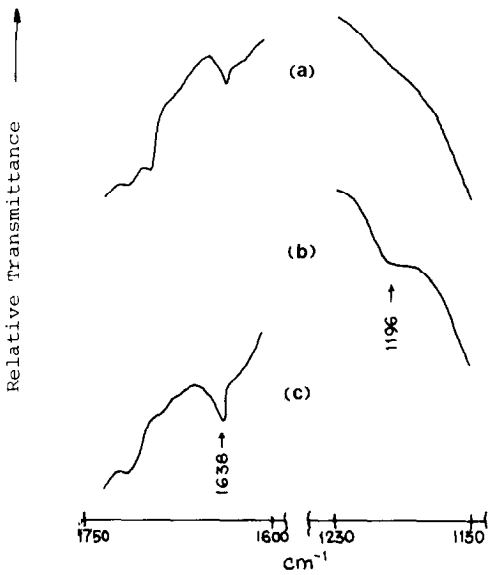

FIG. 8. Infrared spectra of adsorbed H_2O and D_2O on CuCl (20 times accumulation, each ×5). (a) CuCl baked at 433 K and pumped to 8×10^{-6} Torr ("background"). (b) CuCl in stage (a) after treatment with 15 Torr H_2O at 433 K, followed by quenching to RT and gradual pressure reduction in the cells to ~0.5 Torr. (c) CuCl in stage (a) after treatment with 15 Torr D_2O at 433 K, followed by quenching to RT and gradual pressure reduction in the cells to ~0.5 Torr.

DISCUSSION

I. SPECIES IN THE tbc/CuCl SYSTEM

Both ESR and ir techniques were applied to study this system. However, the two techniques do not necessarily detect the same species. The term species here are related to either an ESR signal or a chemical group responsible for certain ir bands. Not all the species are necessarily reaction intermediates for tbc dehydrochlorination.

A. Spurious Oxygen Species Present in Pre-equilibrated State

The fact that both the ESR signal (a) and the family of three ir bands at 856, 900, and 916 cm^{-1} diminished in intensity or even disappeared after tbc and heat treatments seems to indicate that they are probably related to a common cause—a surface species that could be removed by chemical or heat treatments. The magnitudes of the ir frequencies suggest that they might be due to some O–Cl species (see, e.g., Ref. (*16*)). It has been shown in previous works (*5*, *6*) and also by our recent electrical conductivity measurements[2] (*7*) that the CuCl sam-

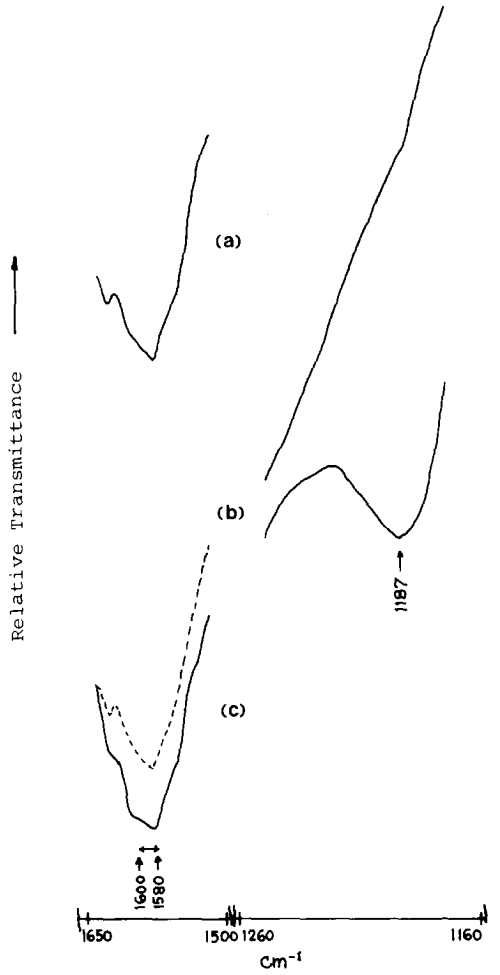

FIG. 9. Infrared spectra of adsorbed H_2O and D_2O on $CuCl_2$ (20 times accumulation, each ×5). (a) "Virgin" $CuCl_2$ ("background"). (b) "Virgin" $CuCl_2$ after treatment with 15 Torr H_2O at 393 K, followed by quenching to RT and gradual pressure reduction in the cells to ~0.5 Torr. (c) "Virgin" $CuCl_2$ after treatment with 15 Torr D_2O at 393 K, followed by quenching to RT and gradual pressure reduction in the cells to ~0.5 Torr.

[2] The DC conductivity of our present purified samples showed a magnitude similar to that of a very slightly chlorinated CuCl sample found by Harrison and Prasad (*6*).

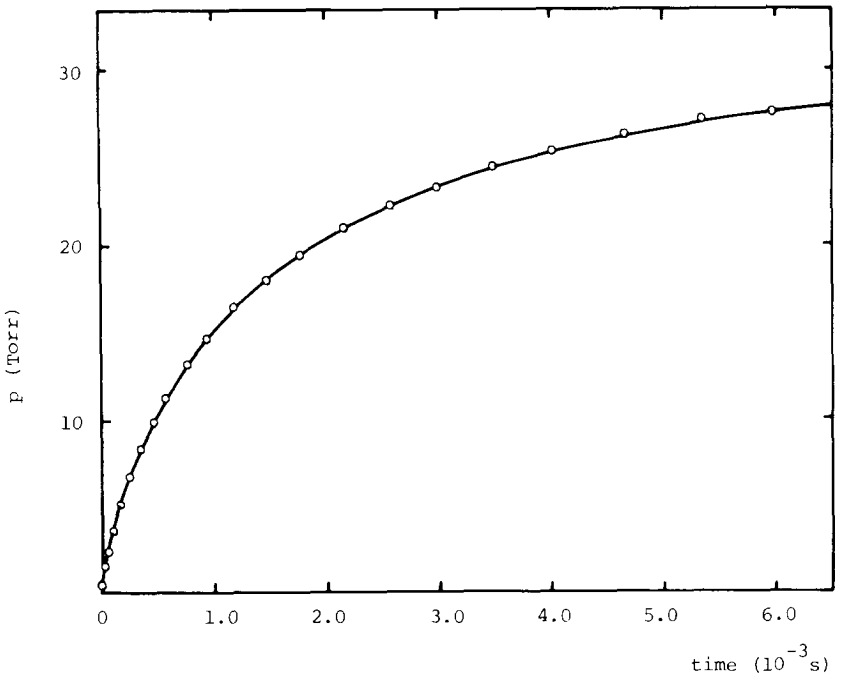

FIG. 10. Pressure change vs time for $CuCl_{1.734}$.

ples used presently would unavoidably contain Cu^{2+} as impurities. Moreover, adsorbed oxygen may cause oxidation of some of the Cu^{+} to Cu^{2+} in presence of trace moisture. Thus the ESR signal (a) might arise from Cu^{2+} under the influence of O^{2-} and Cl^{-} ions on the surface of the solid particles. Such a signal was indeed observed by various workers including one of us (*3*) and no definite assignment appears to have been advanced so far. In this regard, it may be of interest to note that it was proposed that Cu^{2+} ions in divalent zeolites existed in the form of Cu^{+}–O–Cu^{+} linkages (*8, 9*).

The presence of surface oxygen is also supported by the observed release of H_2O by tbc treatments of CuCl as witnessed by the parallel increase in absorption around 3560 and 1620 cm^{-1} in the ir spectrum of the trapped products (Fig. 5). The similarity in the effect exerted by tbc and HCl independently on a CuCl sample (Fig. 4) suggests that the action of tbc owes its origin to HCl produced by tbc dehydrochlorination (The action of HCl may be: $2HCl + O^{2-} \rightarrow H_2O + 2Cl^{-}$). The above deduction is consistent with the kinetic data that for fresh CuCl samples, the dehydrochlorination proceeds much faster in the first one or two runs than the subsequent runs provided the species responsible for ESR signal (a) could impart higher activity in the first one or two runs.

B. Species Present in the "Equilibrated" State

a. Species detected by the ESR method. Since signal (a′) generated by tbc treatments is very broad and resembles that of pure $CuCl_2$, it is likely to arise from Cu^{2+} distributed rather closely together in certain parts of the CuCl lattice. Thus when the surface was "equilibrated" (i.e., cleaned), it contained about $<10^{-6}$ mol% of Cu^{2+} as estimated from signal (a′) of Fig. 1c.

Signal (b), being time dependent as shown in Fig. 3, no doubt is a surface species participating in the tbc dehydrochlorination. Its narrowness and magnitude

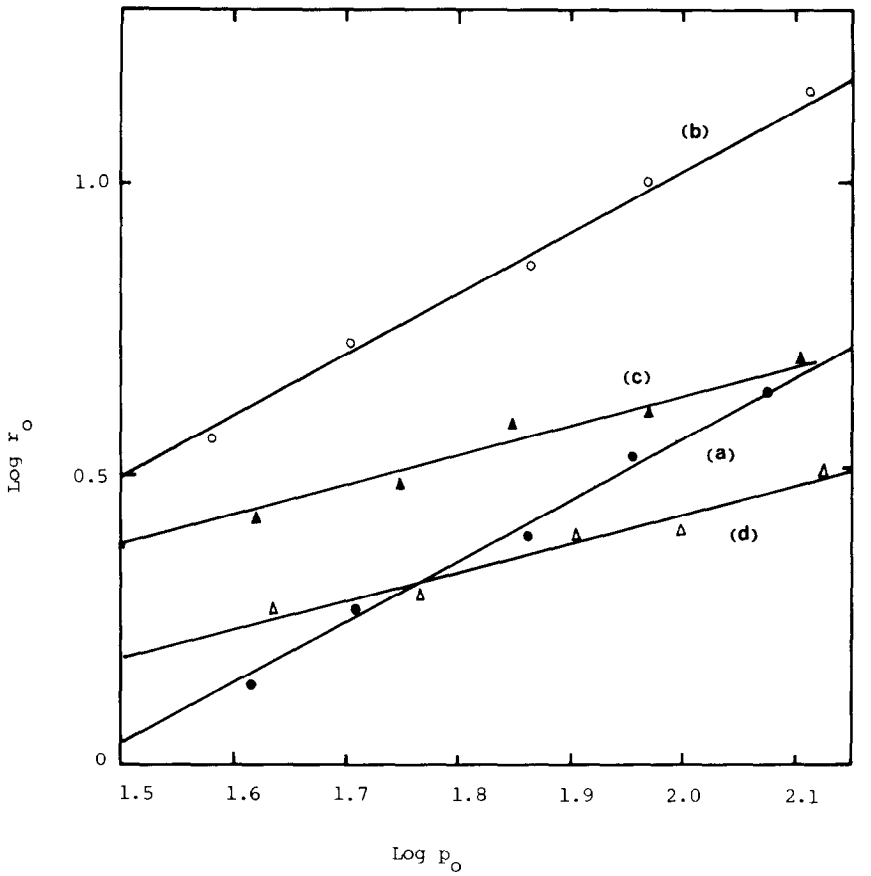

FIG. 11. Establishment of initial order for $CuCl_x$. (a) $x = 1.000$, (b) $x = 1.250$, (c) $x = 1.505$, (d) $x = 1.668$.

of g value suggests that it is associated with a hole trapped defect.

A very similar signal was also observed for $AlCl_3$, $MgCl_2$, and $CdCl_2$ in the course of dehydrochlorination of tbc (*10*). Thus it is tempting to assign this signal to the same species in all these cases viz. chlorine atom interstitials, $Cl_{in(s)}$, acting as hole traps which were proposed in (*5*, *6*) and found by recent electrical conductivity study (*7*) to be the major carrier in nominally pure CuCl at reaction temperature. Possible surface interstitial sites for chlorine atoms are shown in Figs. 15c and d. The g values obtained (CuCl, 2.004; $AlCl_3$, 2.003; $MgCl_2$, 2.005; $CdCl_2$, 2.006) are not too far from those found by Gardner's study (*11*) on the adsorbed chlorine atoms produced by irradiating chlorine treated silica gel, as well as the work of Harrison *et al.* on chlorine atoms by treating NaCl, KCl (*12*), and $SrCl_2$ (*13*) with fluorine, except that a narrower and unresolved peak was obtained in the present work. This could perhaps be explained by the exchange narrowing effect (see, e.g., (*14*)). On the other hand, it is somewhat surprising that the g value of this signal is rather insensitive to the nature of cation. If it were to arise from the same source, it could mean that the true nature of the trap would be something like $[Cl_n]^{(n-1)-}$ involving very little cation orbitals.

As for signal (c), the g value of 2.003 also implies that it is associated with a hole trapped in a defect. Again, this signal was observed in the above three chlorides in the

course of dehydrochlorination. Thus we suggest that it might also arise from a common cause—cation vacancy because the g value is cation insensitive. Once more the absence of hyperfine structure makes assignment uncertain. Nevertheless, this species will be of lesser importance because it apparently did not participate in the chemical reaction.

To understand the interrelationship among various signals which apparently change in magnitude under different experimental conditions, it is perhaps useful to recall the band structure of CuCl. According to the results of electrical conductivity studies (*5–7*), there are at least two types of acceptor levels formed by chlorine interstitials and cation vacancies situated at a distance of ~0.88 and 0.51 eV, respectively, from the top of valence band. Now, a decrease in signal (a) which has been assigned above will probably be due to physical removal of oxygen resulting in the disappearance of the trap related to oxygen (whose energy level though not established yet, presumably lies not too close to valence band because signal (a) was observable at fairly high temperature). The holes released therefrom will serve to increase the concentration of other types of holes present in the system. Indeed, it can be seen from Table 1 that signals (b) and (c) grew when signal (a) diminished to yield signal (a′) (actually, the signal (a) and (a′) had very similar g values and, at some stages of sample treatment, the resulting ESR spectrum was formed by the two signals superimposing on each other). These results, therefore, appear to be consistent if signal (b) is assigned to surface chlorine interstitials, signal (c) to cation vacancies, and the broad signal (a′) to Cu^{2+} in the surface region of CuCl lattice. That signal (c) decreased significantly after cycles of treatment of *tert*-butyl chloride suggests that a diffusion process has taken place. This is also consistent if signal (c) were due to cation vacancy which could undergo diffusion to surface whereby it became annihilated. On the other hand, the return of signal (b) to a maximum after the reaction products were removed and the system was evacuated and baked appears to suggest that the system had reached the "equilibrated" state where signal (b) and signal (a′) are predominantly present and at equilibrium with each other.

The changes of signal (b) and (a′) during the reaction can now be readily understood. Figures 2 and 3 suggest that at the early stage of reaction, $Cl_{in(s)}$ is consumed and at a later stage signal (a′) grew slightly; this is the most relevant information from ESR study in so far as reaction mechanisms are concerned as will be seen later. It should also be noted that the energy change from a Cl_{in} to Cu^{2+} would be <0.88 eV according to the present band structure.

b. Species detected by ir. The elimination reaction of an alkyl halide on a polar catalyst is normally envisaged to proceed through an associative or dissociative adsorption involving bonding of a hydrogen atom and the chlorine atom of the gas molecule to the anion and cation site of the surface, respectively (see, e.g., Ref. (*2*)). If the dehydrochlorination considered also follows such a pattern, the characteristic ir frequencies of the *tert*-butyl group, which is no longer existent in the strict sense, would be expected to be lost or greatly disturbed. On the other hand, if the $CuCl_x$ catalyst were indeed to involve defects, a surface hydrogen and a surface *tert*-butyl group exhibiting the characteristic ir frequencies might well be present. The following discussion will show that these expectations were borne out by experimental results.

Surface tert-*butyl group.* Since rough vacuum reduced significantly the intensity of all the bands observed, the adsorbed species resulting from tbc adsorption on CuCl apparently involve fairly weak interaction with the surface (Figs. 6b and c). The absence of any band in the C=C stretch range—region (B), and the intense characteristic δ-CH out of plane deformation band of isobutene (being 890 cm^{-1} for gaseous isobutene) suggest that isobutene, a reac-

tion product, was probably not or at most only slightly adsorbed on CuCl under the experimental conditions. Auxiliary evidence for this is that isobutene alone was found to yield a surface species of barely sufficient amount to give detectable δ-CH out of plane deformation band near 886 cm^{-1}—almost identical with the corresponding gaseous isobutene frequency as illustrated in Fig. 6e.

Therefore the C–H stretch bands (2975–2870 cm^{-1}) observed in region (A) (Fig. 6) might safely be attributed to adsorbed tbc species only. It follows that the five bands 2975, 2962, 2949, 2910, and 2870 cm^{-1} might be reasonably regarded as the counterparts of the family of five bands in the C–H stretch region for gaseous tbc viz. 2990, 2979, 2960, 2922, and 2870 cm^{-1}, respectively. Amongst these five bands, 2990 and 2870 cm^{-1} are well known to be the asymmetric ν-CH_3 stretch and symmetric ν-CH_3 stretch whereas the rest are probably due to overtone and combination of some low-frequency modes or interaction between the two stretch modes. If this correspondence were accepted, then the small negative shift in the asymmetric stretch and the virtually unaffected symmetric stretch frequency appear to suggest that the adsorption of tbc on the CuCl surface results in such a *tert*-butyl species that the motions of its methyl groups are only weakly perturbed by the surface in comparison with those in a *tert*-butyl group belonging to a gas molecule such as tbc. A diagnostic test for the existence of a *tert*-butyl surface species actually comes from the presence of a pair of bands in region (D). The bands at 1245 and 1165 cm^{-1} should owe their origins to the skeletal C–C stretch mode E and A_1, respectively, characteristic of a hydrocarbon containing a *tert*-butyl group (*15*) quoted in most reference books as 1250–1200 and 1200 cm^{-1}. Actually, the corresponding frequencies of gaseous tbc are 1242 and 1161 cm^{-1}. This means that the CuCl surface renders a reduction in the symmetric C–C stretch similar to that by Cl in tbc (~40 cm^{-1} as compared with a hydrocarbon group). This point will be addressed again later.

The four bands in region (C) probably arise from two pairs of frequencies due to asymmetric CH_3 scissoring and symmetric CH_3 scissoring, respectively, again consistent with a *tert*-butyl surface species.

Finally, further strong evidence for a surface *tert*-butyl species is the absence of the strong C–Cl stretch band in region (E), suggesting that the chlorine atom is no longer part of the original molecule.

Surface hydrogen. Since hydrogen chloride is a product of the reaction, it is of interest to look for the existence of surface hydrogen. Our results show quite clearly the absence of a M–H stretch band in region (B). On the other hand, a weak band observed around 2804 cm^{-1} after tbc was subjected to reaction conditions could perhaps be speculated to arise from an adsorbed hydrogen through the surface chloride ion (this band was not observed when tbc was adsorbed at room temperature as shown in Fig. 6d). Incidentally, since the characteristic doublet of hydrogen atom was not observed in our ESR study, the surface hydrogen proposed here would have to be a proton.

II. Surface Species in the tbc/$CuCl_2$ System

In this case, only ir and kinetic data are available. The ir bands in general were weaker than those observed for CuCl, suggesting the adsorption for various gas species on $CuCl_2$ is probably weaker than that of tbc on CuCl surface. This is also reflected by the small adsorption constants calculated from the kinetic data of the $CuCl_x$ system as described later.

Adsorbed Isobutene

As shown in Fig. 7e, isobutene was clearly adsorbed on $CuCl_2$. So unlike the case of CuCl, it appeared desirable to have a knowledge of ir spectra of adsorbed iso-

butene in detail before the ir data of adsorbed tbc is interpreted.

While the presence of the band at 1580 cm^{-1} implies that the C=C double band character of isobutene is retained, its interaction with the surface is nevertheless fairly strong judging by a low shift of this frequency by ~80 cm^{-1} from that of gaseous isobutene.

The band at 3060 cm^{-1} should correspond to the C–H stretch of the $=CH_2$ group, i.e., the 3080 cm^{-1} band in gaseous isobutene. The broad feature in the 2959–2836 cm^{-1} range in which the background shows considerable absorption makes the assignment of band positions difficult. All that can be said is that absorption in this range might be related to the 2960 and 2890 cm^{-1} of the gaseous isobutene. The band at 2755 cm^{-1} appears too low for C–H stretch. But its exact origin is obscure.

The band at 1430 cm^{-1} and the shoulder at 1374 cm^{-1} might actually be two unresolved bands due to the asymmetric and symmetric CH_3 scissoring modes. The failure to observe bands in region (D), on the other hand, might be due to insufficient intensity as their counterparts in gaseous isobutene are only moderately intense. Finally, the supposedly intense and characteristic out of plane deformation mode could not be studied because of the very steep background absorption in the region below 1000 cm^{-1} as can be appreciated from spectra in region (D) shown.

Surface tert-Butyl Group

Though the absence of a C–Cl stretch band about 810 cm^{-1} could not be ascertained because of steep background absorption just mentioned, the presence of two bands at 1257 and 1202 cm^{-1} (Figs. 7b and c) can again be considered diagnostic of the existence of a *tert*-butyl group. Since both adsorbed *tert*-butyl group and isobutene give rise to several bands in the C–H stretch region, the complicated spectrum observed is not surprising. The positions of bands for the *tert*-butyl group would better be derived from spectrum 7d obtained for tbc adsorption at ambient temperature on the assumption that they would not be significantly altered by the simultaneous presence of isobutene in the course of actual reaction. Thus the shoulder about 2960 cm^{-1} might be associated with the asymmetric C–H stretch of the methyl groups. On the other hand, the band near 2918 cm^{-1}, being most intense and persistent to evacuation, might possibly correspond to the 2949 cm^{-1} band observed for CuCl (Fig. 6c)—a low shift of ~30 cm^{-1}. Since it can be seen from Figs. 6 and 7 that there is a general low shift of the envelope of bands due to *tert*-butyl group in going from CuCl to $CuCl_2$, it seems fair to expect that the asymmetric ν_{CH_3} stretch band in the case of $CuCl_2$ would also be low shifted by about 30 cm^{-1} from that in the CuCl case, i.e., occurring about 2945 cm^{-1}. This is to be compared with the 2960 cm^{-1} band detected. Considering the background absorption and poor resolution of the observed bands, it appears reasonable to consider the frequency in question to be in the neighborhood of these two values. With reference to gaseous tbc, this amounts to a low shift of 30–40 cm^{-1}, suggesting that the C–H stretch frequency in the methyl groups is affected by adsorption slightly more strongly in the case of $CuCl_2$ than in the case of CuCl (a difference of 15–25 cm^{-1}). This point will be dealt with further when mechanisms are discussed.

As for the two skeletal bands 1257 and 1202 cm^{-1} (Fig. 7b, region (D)), it is interesting to note that the magnitude of the A_1 mode (the latter band) is very close to that exhibited by a hydrocarbon containing a *tert*-butyl group, in contrast to that of tbc and adsorbed *tert*-butyl group on CuCl. The magnitude of this parallel vibrational mode has been shown to be more sensitive than that of the perpendicular E mode toward the mass of the hydrocarbon group that connects to the *tert*-butyl group (*15*). The insensitivity of the E mode has also been

borne out by our own ir results. As for the A_1 mode, since the mass factor should be the same for both CuCl and $CuCl_2$ surfaces, a difference of ~40 cm^{-1} in this frequency must be due to some other properties of the adsorbing site. It follows that the adsorbing site in CuCl seems unlikely to be an ordinary Cu_s^+ surface ion. Indeed as will be discussed later, it is possible to deduce that Cu_s^{2+} ions may be produced on the CuCl surface and act as adsorbing sites when other data are viewed together.

Finally, the pair of bands appearing in region (C) of spectrum 7c should correspond to probably unresolved CH_3 scissoring modes of the *tert*-butyl group.

Surface Hydrogen

It was pointed out earlier that the angle bending frequency of adsorbed H_2O would probably be close to 1580–1600 cm^{-1}, judging by the shape of the spectrum shown in Fig. 9. On the other hand, adsorbed D_2O shows a clear absorption band at 1187 cm^{-1}; the corresponding H_2O band could therefore be roughly estimated to be ~1605 cm^{-1} from a consideration of gas, liquid, and solid phase of D_2O and H_2O spectra (*16*). Hence, the observed 1626 cm^{-1} band in spectra 7b and 7c is unlikely to be related to adsorbed H_2O. A copper hydrogen stretch mode, however, could possibly be its origin. The relatively high resistance to evacuation of this band suggests that the species might be relatively stable. On the other hand, it should be pointed out that in view of the weak and broad nature of the bands in region (A), it is less certain whether a $\overset{H}{\underset{\vdots}{Cl_s}}$ species is absent or not.

III. Mechanisms of tbc Dehydrochlorination on $CuCl_x$

In discussing the kinetic mechanisms of $CuCl_x$, it is useful to recall that in dehydrochlorination, the C–Cl bond is easier to break than the C–H bond and that radical intermediate is deemed less favorable than spin paired intermediate, i.e., heterolytic fission of bonds is preferable to homolytic fission in general (*2*).

In Part I (*1*), we have shown that there are two distinct sets of order and activation energy for dehydrochlorination of tbc on the $CuCl_x$ system, and that the prominent double-peak activity pattern observed might be related to the amount of Cu_F^+ ions migrated from the CuCl to the $CuCl_2$ phase. It is, therefore, logical to consider at the outset several composition ranges when discussing the kinetics and mechanisms.

A. Mechanism Scheme I—$CuCl_x$ with $2.00 \geq x \geq 1.25$

As discussed in Part I (*1*), the reaction in this range of composition is predominantly in the $CuCl_2$ phase. It is also the range where the double-peak pattern of the catalytic rate corresponding to the maximum number of Cu_F^+ is found. The kinetic data of each sample yield a reaction of order one-half with respect to *tert*-butyl chloride and this clearly invokes dissociative adsorption and that the rate-determining step is a surface reaction involving part of the dissociated reactant. As for $CuCl_2$ itself, since its activation energy is similar to those obtained for other members of this range and the kinetic data fit fairly well to Eq. (1) described later, it seems that the same mechanism may be operating possibly because the samples did contain certain amount of Cu_F^+ ions that might be favorably distributed on the surface. It follows that the ir data obtained for the $CuCl_2$ case will be relevant in considering the reaction mechanism for catalyst samples with composition in this range. Thus assuming the surface *tert*-butyl group and the surface hydrogen bonded to a copper ion observed in ir study to be possible reaction intermediates, a compatible mechanism that accommodates the effect of Cu_F^+ as well could be proposed.

From X-ray data (Part I), it was deduced that Cu_F^+ ions might occupy vacant octahedral or tetrahedral sites in the $CuCl_2$ lattice. These are represented as type A and type C in Figs. 15a and b, respectively. Actually, there is a third type of sites (type B in Fig. 15a) that may accommodate a Cu_F^+ ion—an octahedral hole situated between two Cu^{2+} ions in a chain. However, such sites would probably be unimportant as they should be at best scarcely populated because their filling would obviously involve rather great steric hindrance and would not result in the observed changes in the lattice parameters of $CuCl_2$. While both Cu_F^+ of type A and C could be utilized, type A offers itself readily for a mechanism that is consistent with all data available so far. Therefore, we envisage the active center for tbc dehydrochlorination to be a triangle consisting of one $Cu_{F(s)}^+$ and two nonequivalent Cu_s^{2+} ions (I and II) on an exposed {100} plane as shown in Fig. 15a.

The mechanism involving such an active center can now be described with the aid of Fig. 12. The first step is adsorption onto Cu_s^{2+} sites followed by a slow surface reaction step that splits off hydrogen atom from the *tert*-butyl radical. The third step is the release of products from the surface. The action of Cu_F^+ may be twofold. A surface $Cu_{F(s)}^+$ ion could possibly donate an electron to promote extraction of chlorine so as to form a radical and a chloride ion (a step making use of the high electron affinity of chlorine). Consequently one has something in between homolytic and heterolytic splitting of the C–Cl bond. Such "pseudo-heterolytic" fission should be energetically favorable because of transfer of electron to a chlorine atom and the relatively stable species $\geqslant C^{\cdot}-Cu_s^{2+}$ (compared with a carbonium ion) may compensate for the energy requirement of the bond breaking process. In fact, without the presence of $Cu_{F(s)}^+$ ions, the conventional acid base catalytic elimination involving chlorine being attached to the acidic site (i.e., Cu_s^{2+}) and an hydrogen attached to the basic site (i.e., Cl_s^-), will more likely be followed.

The second function of Cu_F^+ may be to initiate proton transfer making use of the variability of valence of Cu^{2+} ion, as schematically shown (process marked (**) in Fig. 12) and thereby reduce the rate of recombination of $(\geqslant C{=}CH_2)_{ads.}$ and $H_{ads.}^+$. It should be noted that to participate in this relay, the Cu_F^+ need not be those confined to the surface. This kind of proton transfer was first proposed in the earlier consideration of chlorination of propane (*17*).

On the basis of this proposed mechanism, it can be readily shown that the rate equation for the reaction is

$$r = LL' \frac{k_2 K_A p_A - k_2' K_R K_{HCl} p_R p_{HCl}}{[(K_A p_A)^{1/2} + K_{HCl} p_{HCl}][1 + 2(K_A p_A)^{1/2} + K_R p_R]} \tag{1}$$

where L and L' are the concentration of surface sites for Cu_s^{2+} and $Cu_{F(s)}^+$, respectively; p_A, p_R, p_{HCl} are the pressure of *tert*-butyl chloride, isobutene, and hydrogen chloride, respectively; K_A, K_R, K_{HCl} are the adsorption equilibrium constant of *tert*-butyl chloride, isobutene, and HCl, respectively; and k_2 and k_2' are the forward and reverse rate constant. On rearranging (1) and letting

$$k = LL' k_2 K_A^{1/2},$$

$$k' = k_2' K_R K_{HCl} LL' K_A^{-1/2},$$

$$K_1 = K_A^{1/2},$$

$$K_2 = K_{HCl} K_A^{-1/2},$$

$$K_3 = K_R,$$

$$p_0 - p = p_A$$

and

$$p = p_R = p_{HCl},$$

then

$$r = \frac{k(p_0 - p)^{1/2} - k'p^2/(p_0 - p)^{1/2}}{\left[1 + K_2 \dfrac{p}{(p_0 - p)^{1/2}}\right][1 + 2K_1(p_0 - p)^{1/2} + K_3 p]}. \tag{2}$$

The constants in Eq. (2) can be found by a simple method as described in the Appendix.

A typical solution (demonstrated by various plots corresponding to Eqs. (2B), (2C), and (2D) in the Appendix) is shown for the case of $CuCl_{1.734}$ in Fig. 13. The straight line fit in these plots is apparent.

The calculated rate constants and various adsorption constants (K values) for several compositions of $CuCl_x$ in this range are tabulated in Table 5.

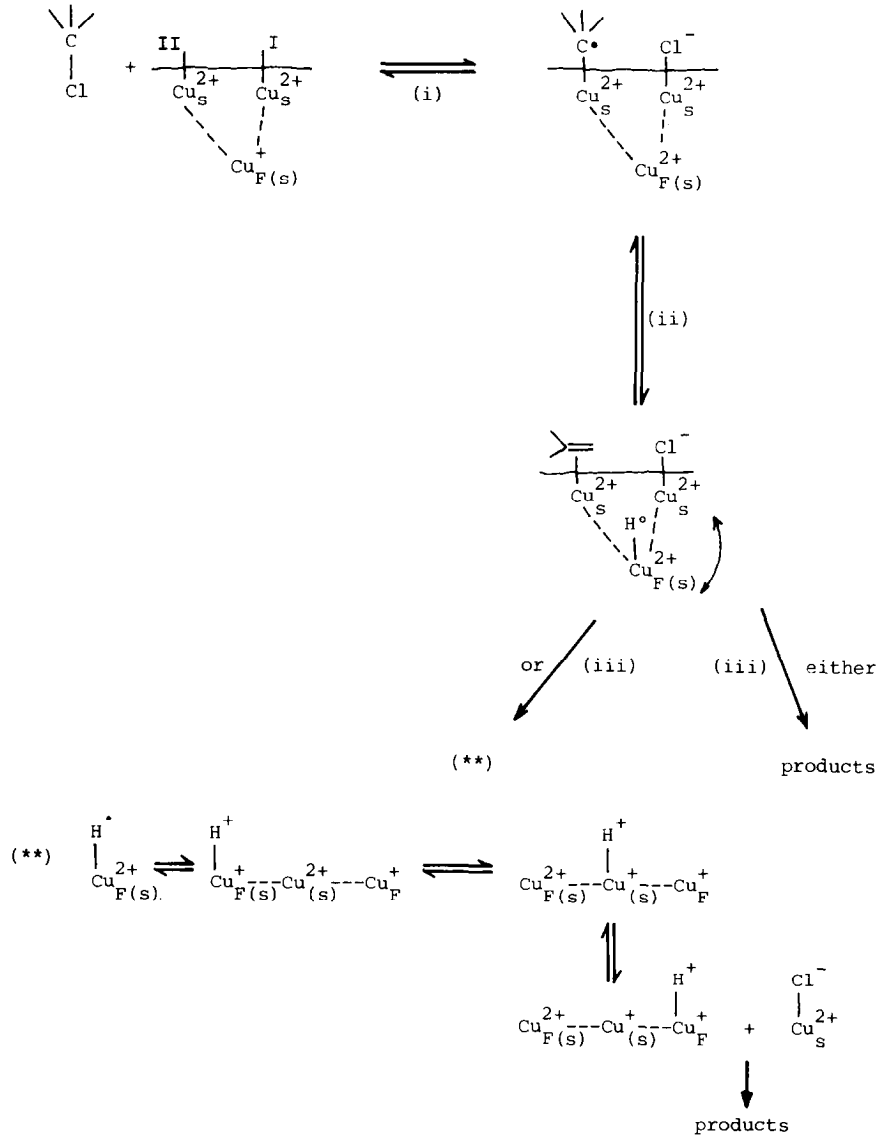

FIG. 12. Mechanism Scheme I—$CuCl_x$ with $2.00 \geq x > 1.25$.

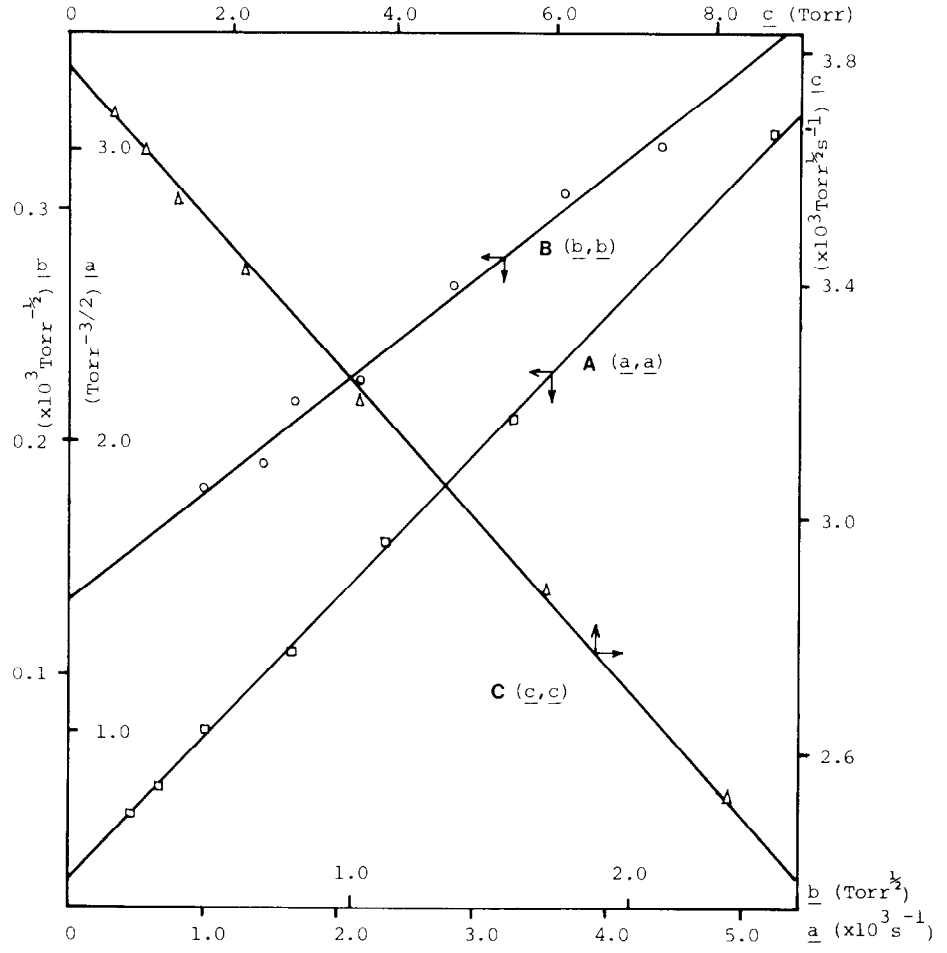

FIG. 13. (A) Determination of K_2 and k': $\frac{(p_0 - p)^{1/2}}{p^2}$ vs $\frac{r}{p}$ (Eq. 2B).

(B) Determination of K_3 and $\left[k(p_0 - p)^{1/2} - k' \frac{p^2}{(p_0 - p)^{1/2}} - r'\right] \frac{1}{r'(p_0 - p)^{1/2}}$ vs $\frac{p}{(p_0 - p)^{1/2}}$ (Eq. 2C).

(C) Final determination of k': $r'[1 + 2K_1(p_0 - p)^{1/2} + K_3 p] \frac{1}{(p_0 - p)^{1/2}}$ vs $\frac{p^2}{p_0 - p}$ (Eq. 2D).

From the above treatment, it can be seen that the experimental data fit the derived rate equation reasonably well. The adsorption equilibrium constants (K_A, K_R, K_{HCl}) are practically the same for all the compositions under investigation. Their low magnitudes suggest amounts of adsorption being small as reflected by intensity of ir absorption bands pointed out earlier. It is also interesting to note that according to the derived rate equation, the rate is directly proportional to the concentration of Cu_F^+ (L') migrated into the $CuCl_2$ lattice from the CuCl lattice. Macroscopically, LL' will of course be incorporated into an apparent forward rate constant $k_{2\,app.}$ and forms an integral part of the frequency factor. Thus over this range of composition, the fact that the activation energy remains unchanged means the change in rate is a consequence of variation of Cu_F^+ concentration in the $CuCl_2$ phase in concurrence with findings as discussed in Part I (*1*).

Before closing this section, two points

TABLE 5

Rate and Adsorption Constants of $CuCl_x$

X	k (Torr$^{1/2}$ s^{-1}) ($\times 10^{-3}$)	k' (Torr$^{-1/2}$ s^{-1}) ($\times 10^{-4}$)	K_A (Torr^{-1}) ($\times 10^{-7}$)	K_R (Torr^{-1}) ($\times 10^{-4}$)	K_{HCl} (Torr^{-1}) ($\times 10^{-4}$)
2.000	2.88	1.37	6.96	7.38	7.78
1.796	2.53	1.22	6.41	7.01	8.56
1.734	3.72	1.78	6.56	7.70	8.18
1.668	2.43	1.17	6.30	7.65	8.34
1.505	3.77	1.83	5.90	7.90	7.91

deserve comments. First, our data do not positively rule out the possibility of type C or type B Cu_F^+ ion (if sufficiently present) being part of an active center. Second, even though type C and type B Cu_F^+ ions might not contribute to reaction rate, they could still be responsible for other kinds of physicochemical properties.

B. Mechanism Scheme II—"Pure" CuCl

It has been suggested from our ESR results that the CuCl surface in "equilibrated" state contains interstitial chlorine atom $Cl_{in(s)}$ (signal (b)), which is transformed to $Cl^-_{in(s)}$ during reaction. The catalytic reaction of CuCl therefore also involves an electron transfer process. Moreover, in view of the first-order reaction with respect to *tert*-butyl chloride found from kinetic data, the reaction appears to proceed with an initial slow rate determining adsorption step involving electron transfer followed by a relatively fast surface reaction step. Again, assuming the surface species found from ir study to be the likely reaction intermediates as well, a mechanism for this reaction can be proposed and schematically shown in Fig. 14.

Step (i) involves a homolytic splitting of the C–Cl bond on two surface cation sites and electron transfer from a $Cl_{in(s)}$ to a surface Cu_s^+ resulting in a Cu_s^{2+}. In this case, we have a parallel situation when compared with that of the $CuCl_2$ case; the active center now consists of a different triangle—two Cu_s^+ and a $Cl_{in(s)}$. Such a triangle may be provided by various planes of CuCl. Two likely candidates are the {100} and the {111} planes. As can be seen from Fig. 15, the suggested site for $Cl_{in(s)}$ on the {100} plane lays slightly deeper than the surface cation sites and therefore forms an equilateral triangle with two Cu_S^+ ions 3.83 Å apart. On the other hand, the suggested site on the {111} plane is actually one that completes a tetrahedron for a Cu^+ ion underneath; the triangle formed is also equilateral with two Cu_s^+ ions 3.83 Å apart. It may also be mentioned that there are only two kinds of Cu^+–Cu^+ distance in CuCl, viz. 3.83 and 5.41 Å. So even if all planes were exposed, there are only two kinds of triangle that can be formed by introducing a $Cl_{in(s)}$. The Cl^-_{ads} may be stabilized by internal electron transfer from the adsorbing Cu_s^+ to form Cl^-–Cu_s^{2+}. This process is energetical favored due to the high electron affinity of chlorine. On the other hand, ir data suggest that the interaction between the *tert*-butyl group and the CuCl surface is considerably stronger than that occurring on the $CuCl_2$ surface. This in turn seems to suggest that the bonding is unlikely through an ordinary Cu_s^+ ion, as also consistent with the ESR data which did not display the hyperfine structure characteristic of the *tert*-butyl radical. By contrast, if an electron transfer process took place initially, the resulting Cu_s^{2+} ion should be a much stronger adsorption site than an ordinary Cu_s^+ ion because it is doubly charged. Indeed, from electronegativity consideration, it is reasonable to expect that its adsorption strength for the *tert*-butyl group should be even stronger than a Cu_s^{2+} on $CuCl_2$ surface because it has nominally only three neighboring Cl^- ions whereas the latter has nominally five neighboring Cl^- ions. This was actually borne out by experiments; not only ir but also kinetic data show that the adsorption was stronger in the CuCl case.

Step (ii) is the transfer of a proton to the newly formed $Cl^-_{in(s)}$ and the release of iso-

[2] This value changes slightly with x value in $CuCl_x$, see Part I (*1*).

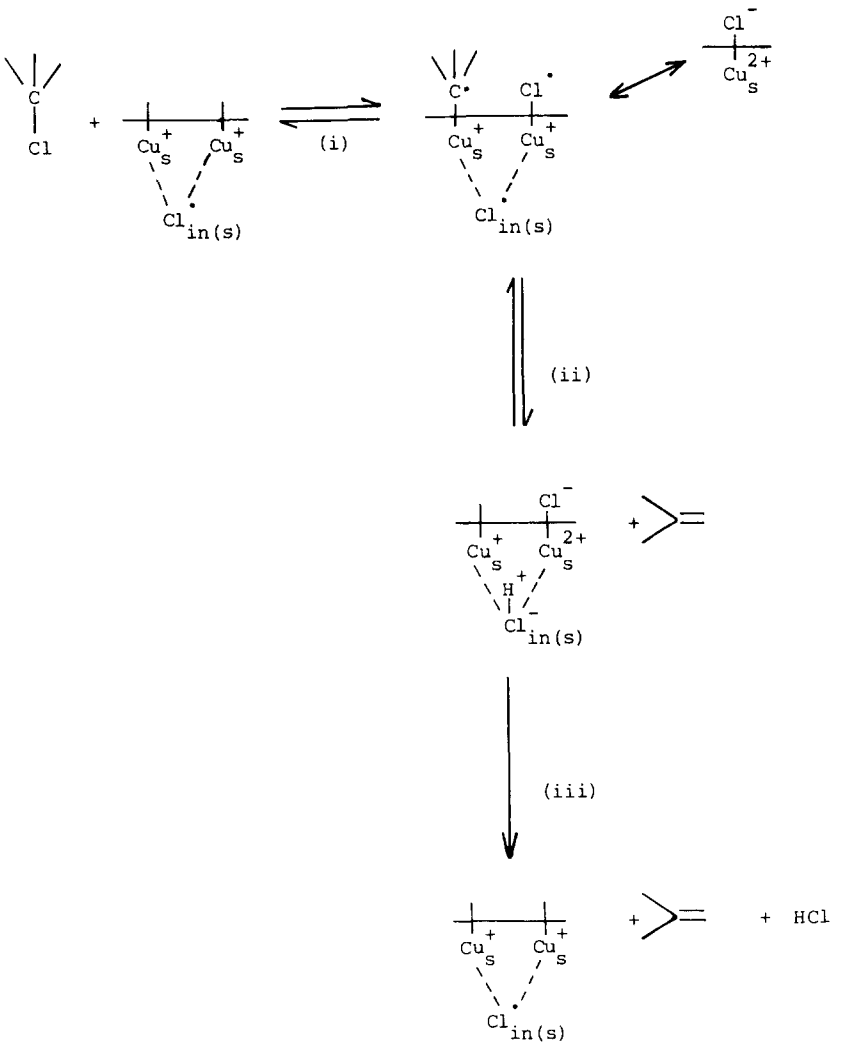

FIG. 14. Mechanism Scheme II—"pure" CuCl.

butene. This proposal is based on the ir data that a surface hydrogen bonded to a Cl_s^- ion was present and that isobutene was hardly adsorbed on the CuCl surface.

Step (iii) is the release of HCl and regeneration of $Cl_{in(s)}$ species.

On the basis of the foregoing mechanism, the rate equation can readily be derived as:

$$r = \frac{L^2}{\left(1 + \frac{1}{K_1} K_R^2 p_R^2 + 2K_R p_R + \frac{K_{HCl} p_{HCl}}{K_R p_R}\right)^2} \left[k_a p_A - \frac{k'_a}{K_1} K_{HCl} K_R p_{HCl} p_R\right] \quad (3)$$

and the initial rate (r_0) is given as

$$r_0 = L^2 k_a p_0 \quad (4)$$

where the symbols in Eqs. (3) and (4) are defined similarly as in the case of $CuCl_2$.

From Eq. (4), it can be seen that the reaction is first order with respect to *tert*-butyl chloride, which was indeed observed ex-

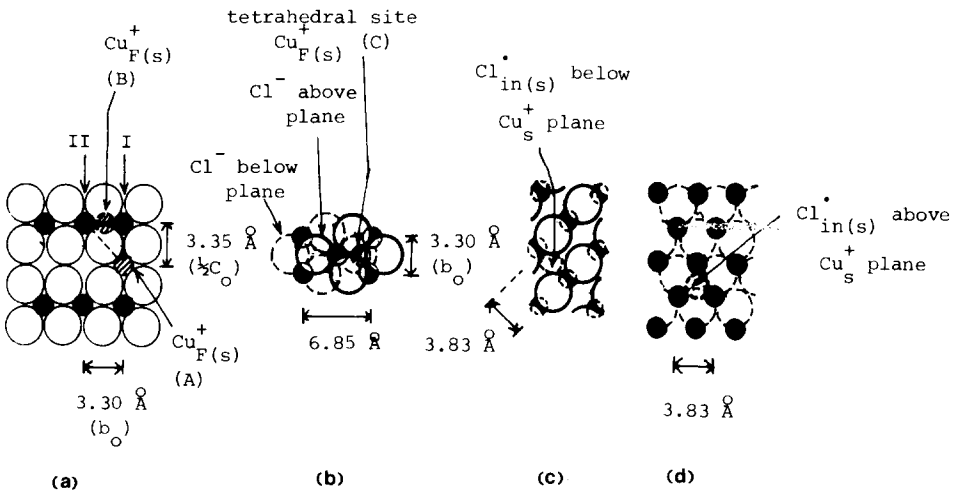

FIG. 15. Possible active centers for dehydrochlorination in CuCl and $CuCl_2$ phase (all interatomic distances shown are those for undistorted lattices). (a) (100) plane of $CuCl_2$ (I and II lattice copper ions nonequivalent, A, B are two types of copper interstitial sites). (b) (001) plane of $CuCl_2$ (type C copper interstitial shown). (c) (100) plane of CuCl. (d) (111) plane of CuCl (the three Cu_s^+ surrounding $Cl^{\bullet}_{in(s)}$ are equivalent and can give rise to three equally probable triangles).

perimentally. However as the rate equation is complicated by the existence of different powers in p_R, detailed calculations using the experimental data are not possible except by the iteration method using a computer. No attempt was made to solve the equation as only marginal information could be gained by doing so.

C. Mechanism for $CuCl_x$ with $1.25 > x > 1$

Though the catalytic activity in this range of composition is predominantly due to the CuCl phase as previously pointed out, the kinetics are more complicated due to the participation of the more active $CuCl_2$ phase present in the catalyst. In view of the reaction order and activation energy, the mechanism is believed to be similar to the case of CuCl, however, the rate of reaction will surely be affected by the $CuCl_2$ present. Hence the rate equation will not be a straightforward one, and no detailed analysis has been attempted.

It should be noted that rate equations with similar numerators but different denominators to those of Eqs. (1) (2) could also be derived on the basis of a conventional polar catalyst mechanism. Thus, it is only marginally possible to differentiate between the defect mechanisms and conventional mechanism by kinetic data fitting alone.

Before we conclude, it may now be appreciated that the two different kinds of interstitials result in two apparently similar but actually quite different *tert*-butyl surface species. Apart from the electronegativity of the adsorbing Cu_s^{2+} concerned which has been discussed, the interionic distance between the two Cu_s^{2+} of the suggested triangular active center in $CuCl_2$ case is ~0.53 Å shorter than the corresponding value in CuCl case. Consequently, the adsorbed *tert*-butyl group might be closer to other adsorbed species in the $CuCl_2$ case, resulting in a larger perturbation of the C–H stretch of the methyl group as borne out by the relatively larger low shift of the asymmetric ν_{CH_3} stretch frequency.

CONCLUSIONS

Attempts were made to use ESR and ir techniques to identify reaction intermediates in tbc dehydrochlorination on $CuCl_x$.

Four ESR signals were observed for the tbc/CuCl system. They were found to undergo changes by cyclic tbc treatments, two of which were found to change in a reproducible manner on an "equilibrated" sample in the course of dehydrochlorination. The nature of species associated with these signals was tentatively suggested, one of which viz. $Cl_{in(s)}$ was identified as a probable reaction intermediate for tbc dehydrochlorination.

Infrared data enable us to deduce that a *tert*-butyl group bonded to a surface copper ion is present on both CuCl and $CuCl_2$ surfaces during tbc adsorption and probably dehydrochlorination. Moreover, in the former case, hydrogen was possibly adsorbed onto the surface anion and isobutene was virtually nonadsorbed under conditions similar to that of reaction. In the latter case, hydrogen was possibly adsorbed onto the cation while isobutene adsorption was found to take place. Thus both surface *tert*-butyl and surface hydrogen were also likely reaction intermediates for tbc dehydrochlorination.

On the basis of ESR and ir findings, together with other information including the additional kinetic results reported in this paper, two different defect mechanisms of dehydrochlorination, applicable to various ranges of composition of the $CuCl_x$ system, were proposed. One involves an active center consisting of a triangle—two Cu_s^{2+} and one $Cu_{F(s)}^{+}$ while the other involves a different triangle—two Cu_s^{+} and one $Cl_{in(s)}$.

Finally, reaction rate equations were derived. The values of rate and adsorption constants were calculated for samples obeying Mechanism I.

APPENDIX

Procedure for Obtaining Constants in Eq. (2)

(i) Taking initial pressure p_0 with initial rate of reaction r_0 so that

$$r_0 = \frac{kp_0^{1/2}}{1 + 2K_1p_0^{1/2}}$$

then the values k and K_1 can be estimated by using initial rate data. Thus a half-order reaction would be expected if K_1 is small.

(ii) K_1 from (i) is known to be small and assuming $K_3p > 1$, then Eq. (2) can be rearranged as

$$[k(p_0 - p)^{1/2} - r]\frac{(p_0 - p)^{1/2}}{p^2} = K_2\frac{r}{p} + k' \tag{2B}$$

where K_2 and k' can be estimated from a plot of

$$\frac{(p_0 - p)^{1/2}}{p^2} \quad \text{vs} \quad \frac{r}{p}.$$

(iii) Let $r' = r[1 + K_2(p/(p_0 - p)^{1/2})]$, and rearranging Eq. (2) so that

$$\left[k(p_0 - p)^{1/2} - k'\frac{p^2}{(p_0 - p)^{1/2}} - r'\right]\frac{1}{r'(p_0 - p)^{1/2}} = K_3\frac{p}{(p_0 - p)^{1/2}} + 2K_1 \tag{2C}$$

then K_3 can be estimated from this equation

(iv) Finally, further rearrangement of Eq. (2C) leads to

$$r'[1 + 2K_1(p_0 - p)^{1/2} + K_3p]\frac{1}{(p_0 - p)^{1/2}} = k - k'\frac{p^2}{p_0 - p} \tag{2D}$$

where k' can be estimated from the slope of the straight line plot and be compared with that obtained from Eq. (2B). An illustration of this procedure is shown for one sample as mentioned in the text.

ACKNOWLEDGMENTS

We would like to thank Prof. L. G. Harrison for helpful discussions and Drs. Alfred Leung and T. Y. Luk for making available to us their ESR facilities at the Chinese University of Hong Kong.

REFERENCES

1. Ng, C. F., and Leung, K. S., *J. Catal.* **67,** 410 (1981).
2. Noeller, H., and Klading, W., *Catal. Rev. Sci. Eng.* **13,** 149 (1976).
3. Ng, C. F., Ph.D. Thesis, University of British Columbia (1969).
4. Leung, K. S., Ph.D. Thesis, University of Hong Kong (1980).

5. Harrison, L. G., and Ng, C. F., *Trans. Faraday Soc.* **67,** 1810 (1971).
6. Harrison, L. G., and Prasad, M., *Trans. Faraday Soc.* **70,** 471 (1974).
7. Ng, C. F., and Leung, K. S., in preparation.
8. Lunsford, J. H. *Adv. Catal.* **22,** 265 (1972).
9. Uytterhaeven, J. B., Schoonheydt, R., Liangone, B. V., and Hall, W. K., *J. Catal.* **13,** 425 (1969).
10. Ng, C. F., and Leung, K. S., in preparation.
11. Gardner, C. L., *J. Chem. Phys.* **46,** 2991 (1967).
12. Harrison, L. G., Adams, R. J., and Catton, R. C., *J. Chem. Phys.* **45,** 4023 (1966).
13. Harrison, L. G., Catton, R. C., and Rantama, A. K., *Proc. 6th Intern. Sym. Reactivity Solids* 65 (1968).
14. Townes, C. H., and Turkevich, J., *Phys. Rev.* **77,** 148 (1950).
15. Simpson, D. M., and Sutherland, B. B. M., *Proc. R. Soc.* **A199,** 169 (1949).
16. Nakamoto, K., "Infrared Spectra of Inorganic and Coordination Compounds," 2nd ed. Wiley, New York, 1969.
17. Harrison, L. G., and Ng, C. F., *Trans. Faraday Soc.* **67,** 1787 (1971).